



Cite this: *Polym. Chem.*, 2025, **16**, 879

## Preparation of a new class of phosphonated hydrocarbon polymers based on polysulfone†

Philipp Martschin, <sup>a,b</sup> Timo Prölb, <sup>a,b</sup> Andreas Hutzler, <sup>a</sup> Simon Thiele <sup>a,b</sup> and Jochen Kerres <sup>a,c</sup>

The membrane is the heart of an electrochemical cell. Nowadays, PFSA-based materials, e.g., Nafion®, are state-of-the-art in large-scale energy applications. However, PFSA are relatively expensive and give rise to concerns regarding toxic intermediates in the production process. Moreover, their recyclability and their biodegradability are questionable. Thus, there is a strong need to develop alternative materials with comparable or better properties. This study presents a new class of phosphonated hydrocarbon polymers based on commercially available polysulfone Udel (PSU) synthesized by a lithiation reaction. The modified PSUs were subsequently phosphonated by a Michaelis–Arbuzov reaction. All synthesized polymers/ionomers were further characterized by NMR, DSC, TGA, GPC, TEM, and titration. Moreover, the first blend membranes could be produced out of the new class of PSU derivatives. In summary, four different polymers were synthesized, of which three were successfully phosphonated. Starting from the phosphonated species, three different acid-acid blend membranes were manufactured with sufficient ionic conductivity. These novel phosphonic acid group-containing materials are promising candidates for membranes or ionomers in electrochemical applications, like (HT)-PEMFCs, (HT)-PEMWEs, or redox flow batteries.

Received 13th November 2024,  
Accepted 18th December 2024

DOI: 10.1039/d4py01289e

rs.c.li/polymers

### Introduction

Perfluorosulfonic acid polymers (PFSA)s such as Nafion® are considered state-of-the-art membrane material for PEM electrolyzers and fuel cells.<sup>1–3</sup> Despite their ongoing popularity, PFSA membranes have some shortcomings, e.g., bad conductivities above 100 °C due to dwindling hydration,<sup>4,5</sup> high methanol permeability in direct methanol fuel cells (DMFCs),<sup>6–8</sup> toxic production intermediates (TFE)<sup>5</sup> and low tolerances for impurities.<sup>9</sup> Furthermore, those materials consist of per- and polyfluorinated alkyl substances (PFAS) incorporating fully fluorinated methylene (–CF<sub>2</sub>–) or methyl (–CF<sub>3</sub>) groups.<sup>10</sup> Such substances are often labeled “forever chemicals” due to their environmental persistency and high chemical stability.<sup>11</sup> To overcome these problems, many alternative materials were explored in the last decades.<sup>12–19</sup> The alternative materials include hydrocarbon polymers with perfluor-

aromatic moieties because aromatic C–F bonds are much more reactive than aliphatic C–F bonds. For example, aromatic F can be easily substituted by nucleophilic aromatic substitution reactions, e.g., with thiol or amino groups.<sup>20–25</sup> The higher reactivity of aromatic F-containing compounds, compared to perfluoroaromatic compounds, facilitates their degradation, also in the environment.<sup>26</sup> The released F<sup>–</sup> anions can then react with calcium ions present in the soil to form extremely poorly soluble CaF<sub>2</sub>, which no longer poses an environmental hazard. It was shown that polymers with phosphonic acid (PA) groups yield good conductivities for temperatures above the application range of sulfonic acid functionalized polymers. They are used in so-called high-temperature proton exchange membrane fuel cells (HT-PEMFCs) due to the ability of PA to conduct protons even under low humidity.<sup>7,27</sup> However, introducing phosphonic acid groups into a polymer structure is more complex than introducing sulfonic acids.<sup>21</sup> Moreover, while the doping (phosphoric acid (PA) in a polymer matrix) of non-conducting polymers (like polybenzimidazole (PBI)) with phosphoric acid leads to satisfying conductivities,<sup>28–30</sup> the mechanical stability and the leaching of the doped PA during is still considered a challenge for the HT-PEMFC technology.<sup>9</sup>

Different possibilities to phosphonate hydrocarbon-based polymers are described, for example, in ref. 21 or ref. 31. In this work, we want to focus on the method introduced by Atanasov and Kerres<sup>21</sup> and phosphonate the polymer *via* the

<sup>a</sup>Forschungszentrum Jülich GmbH, Helmholtz Institute Erlangen-Nürnberg for Renewable Energy (IET-2), Cauerstraße 1, 91058 Erlangen, Germany.

E-mail: p.martschin@fz-juelich.de

<sup>b</sup>Department of Chemical and Biological Engineering, Friedrich-Alexander-Universität Erlangen-Nürnberg, Egerlandstraße 3, 91058 Erlangen, Germany

<sup>c</sup>Chemical Resource Benefication Faculty of Natural Sciences, North-West University, Potchefstroom 2520, South Africa

† Electronic supplementary information (ESI) available: Additional characterization data of synthesised polymers. See DOI: <https://doi.org/10.1039/d4py01289e>



nucleophilic substitution reaction of a *para*-fluoro atom of a pentafluorophenyl group-containing side chain. One of the advantages of phosphonic acid groups introduced into a perfluoro aromatic moiety is that these phosphonic acid groups are much more acidic than phosphonic acid groups bound to a nonfluorinated aromatic moiety due to the strong electron-attracting ( $-I$ ) effect of the F, which stabilizes the phosphonate anion.<sup>21,32</sup>

Polysulfone Udel® (PSU) was selected as a polymer precursor for synthesizing the phosphonated polymers presented in this study. PSU is a well-known commercial polymer used as a membrane material in a variety of applications.<sup>33–36</sup> It has good film-forming properties, high thermal and chemical resistance, and can be easily modified, making the introduction of phosphonic acid-pendent side chains possible. On the electron-rich aromatic aryl-ether part, PSU can be modified *via* electrophilic aromatic substitution reactions, for example, by chloromethylation or sulfonation.<sup>37</sup> On the other hand, the aryl-sulfone part prefers nucleophilic reactions due to the electron-withdrawing effect of the sulfone group between the aromatic rings, which confers increased C–H acidity on the H atom in *ortho* position to the sulfone bridge.<sup>38</sup> One modification route of the latter reaction type is by H-abstraction *via* an *ortho* metalation reaction using *n*-butyl lithium and subsequent substitution of the inserted metal. An overview of

possible reactions from lithiated PSU (PSU-Li) is shown in Fig. 1.<sup>36</sup> This reaction route is widely used in membrane manufacturing and, therefore used in this study as well.<sup>31,33,35,36,38–49</sup>

The starting polymer PSU was lithiated with *n*-BuLi to achieve the target structures in the first step. In a second step, the lithium was substituted by a perfluorophenylcarbonyl compound, *e.g.* perfluoroacetophenone, in a nucleophilic substitution reaction (Fig. 2). All described steps were performed in a one-pot synthesis.

In this study, the nucleophilic substitution reaction of the lithiated PSU backbone was performed with four different perfluoroaromatic compounds: perfluoroacetophenone, the resulting product abbreviated in the following as (PSUa), and the purely fluoroaromatic compounds pentafluorobenzoylchloride (PSUc), perfluorobenzophenone (PSUb) and pentafluorobenzenesulfonylfluoride (PSUs). The perfluoroaromatic compounds used are shown in Fig. 3.

To yield an ion-conducting polymer, it is necessary to introduce an ion-conducting group to the modified PSU polymers. This work aimed to synthesize a polymeric membrane material for potential use in high-temperature electrochemical applications. Subsequently, the *para*-fluoro atoms were phosphonated by nucleophilic aromatic substitution by reaction with tris(trimethylsilyl)phosphite to attain a proton-conducting

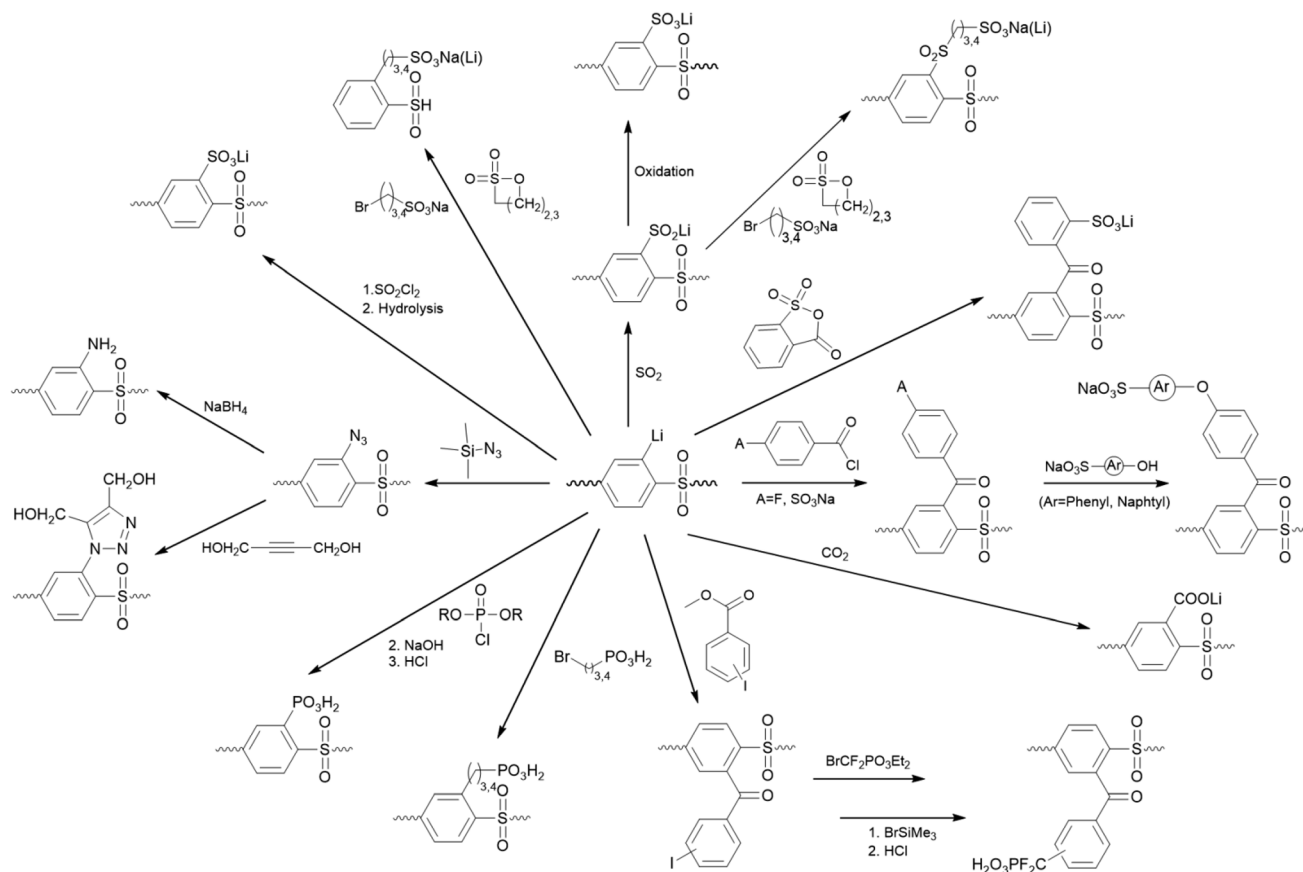


Fig. 1 Possible reactions of lithiated PSU to introduce acid groups.



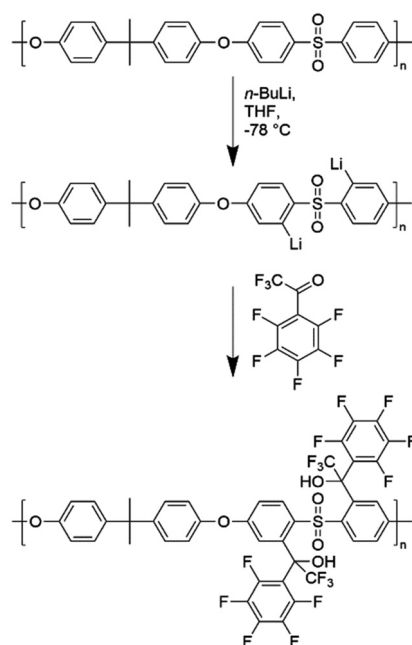


Fig. 2 Scheme of the PSU reaction sequence lithiation – reaction with a carbonyl compound at the example of perfluoroacetophenone.

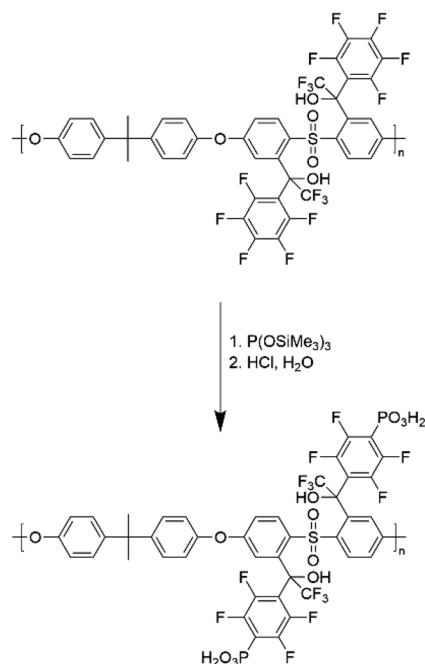


Fig. 4 Exemplary Michaelis–Arbuzov reaction scheme with PSUa to obtain p-PSUa.

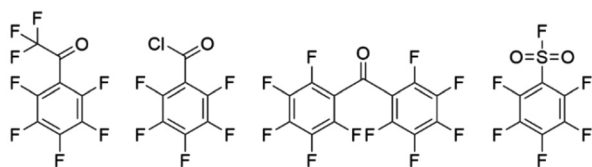


Fig. 3 Used perfluoroaromatic compounds: perfluoroacetophenone (PSUa), pentafluorobenzoylchloride (PSUc), perfluorobenzophenone (PSUb), pentafluorobenzensulfonyl fluoride (PSUs).

polymer after hydrolysis of the silyl ester.<sup>21</sup> This reaction is shown exemplarily in Fig. 4 for PSUa. Afterward, the synthesized materials were fully characterized by NMR-spectroscopy, TGA, DSC, GPC, and acid–base titration.

## Materials and methods

### Materials

Polysulfone Udel® (supplier: Solvay S. A.) or PSU Ultrason S® (producer: BASF SE), respectively, was used as received. Tris(trimethylsilyl)phosphite, perfluoroacetophenone, perfluorobenzophenone, pentafluorobenzoylchloride, and pentafluorobenzenesulfonyl fluoride were purchased at Manchester Organics. *n*-Butyllithium (2.5 M in Hexanes), THF (dry, 250 ppm Butylhydroxytoluene as inhibitor), heptane, and other solvents were purchased at Sigma Aldrich. All chemicals were used without further purification steps. The glassware was cleaned and air-dried prior to use. All syntheses were carried out under an argon atmosphere.

### Instruments, polymer, and membrane characterization

The chemical composition and structure of starting materials and products were characterized by proton, fluorine, and phosphorus NMR-spectroscopy. The  $^1\text{H}$ ,  $^{19}\text{F}$ , and  $^{31}\text{P}$ -spectra were recorded at room temperature by a 500 MHz JEOL ECX-400 NMR spectrometer.

The molecular weight distribution for the non-phosphonated reaction products of lithiated PSU with different perfluoroaromatic compounds and the phosphonated PSU derivatives ( $M_n$ , PDI) was determined using gel permeation chromatography (GPC). In our study, a GPC system SECurity<sup>2</sup> from PSS Polymer Standard Service Mainz, Germany, equipped with a UV and refractive index detector, was used. The chromatography was done with a PSS SDV LUX GUARD, a PSS SDV LUX 3  $\mu\text{m}$  1000 Å, and a PSS SDV LUX 3  $\mu\text{m}$  10 000 Å column set, which were calibrated with a series of polystyrene standards in THF. The respective polymer was dissolved in non-stabilized THF with a concentration of  $1\text{ g L}^{-1}$  for the measurement itself. The polymer solution was filtered using a syringe filter over a microporous PTFE membrane (0.45  $\mu\text{m}$ ), injected, and separated over the columns with a  $1\text{ mL min}^{-1}$  flow rate.

The thermal stability of the synthesized polymers was determined by TGA measurements. For that purpose, a TGA 800 instrument from PerkinElmer was used. The decomposition measurements were performed with a heating rate of  $10\text{ K min}^{-1}$  under a synthetic air (SA) atmosphere, starting from room temperature to  $900^\circ\text{C}$ .

To determine the glass transition temperature ( $T_g$ ) of the synthesized polymers, a DSC 3+ device from Mettler Toledo was used. The sample was heated and cooled down in two



cycles, starting from room temperature up to 300 °C with a heating/cooling rate of 20 K min<sup>-1</sup>.

The ion exchange capacities (IECs) were determined by acid–base titration with an OMNIS Titrator from Metrohm. For the titration itself, the polymers/membranes in H<sup>+</sup> form were stirred in a warm, saturated sodium chloride solution to exchange the protons for sodium cations. The released H<sup>+</sup> ions were titrated with a 0.1 M sodium hydroxide solution to the equivalent point to determine IEC<sub>direct</sub>.

$$\text{IEC}_{\text{direct}} = \frac{\Delta V_{\text{NaOH}} \cdot c_{\text{NaOH}}}{m_{\text{sample}}} \quad (1)$$

Then, a defined volume of 0.1 M sodium hydroxide solution was added. Afterwards, the solution was back titrated with 0.1 M HCl to determine IEC<sub>total</sub>.

$$\text{IEC}_{\text{total}} = \frac{V_{\text{NaOH,excess}} \cdot c_{\text{NaOH}} - [(\Delta V_{\text{NaOH}} \cdot c_{\text{NaOH}}) + (\Delta V_{\text{HCl}} \cdot c_{\text{HCl}})]}{m_{\text{sample}}} \quad (2)$$

The polymer's/membrane's ionic conductivity was measured by impedance spectroscopy with a Zennium X workstation from Zahner, Kronach, Germany. The measurements were done at room temperature in 0.5 M sulphuric acid to minimize contact resistances according to a method described by Kerres *et al.*<sup>50</sup>

The samples' water uptake was determined at 85 °C. The samples were dried in an oven and weighed in a dry state ( $m_{\text{dry}}$ ). Afterward, the samples were placed in a vial with water, which was heated for 48 hours at 85 °C. Then, the samples were taken out of the water, quickly wiped dry, and weighed in the wet state ( $m_{\text{wet}}$ ). The water uptake was calculated based on the two determined values according to the following equation.

$$\text{WU} : \Delta m [\%] = \frac{m_{\text{wet}} - m_{\text{dry}}}{m_{\text{dry}}} \times 100 [\%] \quad (3)$$

The samples' swelling in water was determined at 85 °C. The samples were dried in an oven, and their thickness was measured in a dry state ( $d_{\text{dry}}$ ). Subsequently, the samples were placed in a vial with water, which was heated for 48 hours at 85 °C. Then the samples were taken out of the water, quickly wiped dry, and the thickness was measured in the wet state ( $d_{\text{wet}}$ ). According to the following equation, the swelling ratio was calculated based on the two determined values.

$$\text{Swelling Ratio} : \Delta d [\%] = \frac{d_{\text{wet}} - d_{\text{dry}}}{d_{\text{dry}}} \times 100 [\%] \quad (4)$$

The chemical stability, particularly against radicals, was investigated by storing the samples in Fenton's reagent (4 ppm Fe<sup>2+</sup>, 3% H<sub>2</sub>O<sub>2</sub>) at 85 °C for 48 h. The samples were weighed before and after the test to determine a potential loss in mass.

By using a Thermo Fisher Scientific Talos F200i equipped with a high-angle annular dark field (HAADF) STEM detector, images of a blend membrane were recorded. The microscope features a Schottky emitter and was operated at an acceleration voltage of 200 kV. Data analysis was carried out using the Velox software.

## Polymer modification syntheses

The starting material, polysulfone (PSU), was entirely dissolved in dry THF under an Argon atmosphere at room temperature and cooled down to -78 °C. *n*-Buthyllithium (*n*-BuLi) was added to the solution until all water traces were removed, indicated by a reddish colouring. In the second step, two equivalents of *n*-BuLi per repeating unit PSU were added to the solution, while its colour turned red.<sup>33</sup> After one hour, the respective electrophilic compound (perfluoroacetophenone, perfluorobenzophenone, pentafluorobenzoylchloride, or pentafluorobenzenesulfonylfluoride) was added in molar excess (6 mol of carbonyl per PSU repeating unit). The solution was left stirring at -78 °C until it was homogenized, and then the cooling bath was slowly warmed to room temperature overnight by switching off the thermostat. Subsequently, the polymer was precipitated in methanol and washed with methanol. Finally, the obtained colorless solid was dried under a vacuum.

For the phosphonation according to Atanasov and Kerres,<sup>21</sup> the beforehand modified PSU (PSUa, PSUb, PSUc, or PSUs) was dissolved in pure tris(trimethylsilyl)phosphite and heated up to 160–170 °C under argon atmosphere for several hours. Complete dissolution of the polymer was only obtained at elevated temperatures. If not already precipitated after cooling down, the polymer was precipitated and washed in *n*-heptane.

To remove the silyl esters, the polymer was heated up to reflux in water overnight. After that, the raw product was treated with 1 M HCl for 24 hours at elevated temperature to acidify the phosphonic acid and hydrolyze the intermediate possible remaining silyl ester groups to the H<sup>+</sup>-form of the phosphonic acids (fully protonated form, PO<sub>3</sub>H<sub>2</sub>-group). Finally, the obtained polymer was dried.

## Membrane preparation

For application and measuring conductivity, the polymers were cast as blended membranes. The phosphonated polysulfones (p-PSUa, p-PSUb, and p-PSUs) and the second blend component (a phosphonated terphenyl polymer from *p*-terphenyl and perfluoroacetophenone synthesized by polyhydroxyalkylation and subsequent Michaelis-Arbuzov phosphonation)<sup>51</sup> were dissolved separately in the same solvent and subsequently mixed until a homogeneous mixture was obtained. Afterward, the blend solution was cast onto a glass plate, doctor-bladed, heated to 80 °C, and then the solvent was evaporated in a convection oven. To ensure complete protonation, the membranes were post-treated by immersing them in 10 wt% sulphuric acid at 85 °C for 96 h and washing several times with water at 85 °C until a constant water pH-value of 7 was reached.

## Results and discussion

### Modification of PSU with pentafluorophenyl group containing side chains

**Determination of substitution degree of fluorinated side chains by NMR-spectroscopy.** Virgin PSU was modified in a



two-step, one-pot synthesis. At first, the polymeric backbone was lithiated in an *ortho* position next to the sulfone bridge. Then, the lithium was substituted by one of the four electrophiles mentioned above. The number of side chains introduced per repeating unit of PSU was determined by  $^1\text{H}$  NMR spectroscopy of the respective polymeric reaction product. The lithiated intermediate was not isolated and further characterized. The measured proton NMR spectra of unmodified PSU and modified PSU derivatives are depicted in Fig. 5(a)–(e). To determine the degree of substitution (DOS), the integrals of the protons next to the sulfone bridge were compared to each other. The integrals of these protons with chemical shifts around 8 ppm are smaller compared to those determined in the spectra of pure PSU (Fig. 5(a)) due to the introduction of the perfluoroaromatic side chains. For the non-substituted PSU, the sum of protons in *ortho*-position next to the sulfone bridge is four. Theoretically, it is only possible to substitute two of the four protons by a side chain due to sterical hindrance. The degree of substitution (DOS) can be calculated according to eqn (5), with a 100% DOS equal to two side chains per repeating unit.

$$\text{DOS}_{\text{NMR}} = 1 - \frac{\text{non substituted protons next to sulfone bridge}}{\text{maximum number of substitutable protons next to sulfone bridge} (= 2)} \quad (5)$$

The degrees of substitution, experimentally determined and calculated by  $^1\text{H}$  NMR spectroscopy for the four different used perfluoroaromatic-modified PSU polymers are summarized in Table 1. In comparison, the DOS for PSUa, PSUb, and PSUc are in the same range. However, the DOS for PSUs is markedly lower.

For the substitution reaction of lithiated PSU with pentafluorophenyl compounds, a maximum of two side groups per repeating unit is theoretically possible, resulting in a DOS of 100% (two side chains per repeating unit). A higher theoretical DOS is impossible because the two aromatic rings pendent to the sulfone bridge of the PSU repeating unit become deactivated after the first carbanion per aromatic ring has formed by deprotonation with *n*-BuLi. However, a DOS of one could not be reached in reality for one or more of the following reasons: depending on the introduced pentafluorophenyl compound, the polymer can run into a solubility issue during the substitution reaction. When fluorinated side groups start to become attached to the backbone, the solubility of the polymer in the solvent decreases significantly, or, in other words, the polymer begins to precipitate during the substitution reaction, which prevents complete substitution. This issue was particularly observed at the formation of PSUs (reaction of lithiated PSU with pentafluorophenylsulfonyl fluoride). Furthermore, there is some sterical hindrance after the first side group has been added to the polymer repeating unit. As a consequence, the substitution with a second side group is less probable.

The successful introduction of a perfluoroaromatic side chain was further verified by  $^{19}\text{F}$  NMR spectroscopy (Fig. 6).

The pentafluorophenyl side chains cause a characteristic substitution pattern of the F substituents, resulting in three signals with an integral ratio of 2 : 1 : 2, corresponding to the *ortho*, *para*, and *meta* positions of the fluorine atoms in the pentafluorophenyl moiety. These three characteristic signals show a chemical shift between  $-130$  ppm and  $-170$  ppm. In case there is a  $\text{CF}_3$  group remaining after the substitution reaction (see the conversion of PSU to PSUa), these fluorine atoms are detected at a chemical shift of  $-73$  ppm. However, the DOS cannot be determined from the  $^{19}\text{F}$  NMR spectra because there is no fluorine in the unmodified PSU as a reference. It is only possible to check by  $^1\text{H}$  NMR whether the substitution reaction was successful.

**Phosphonation of the obtained PSU-derivatives.** To yield an ion-conducting polymer, a phosphonic acid group was introduced *via* a Michaelis–Arbuzov reaction at the pentafluorophenyl groups.<sup>21</sup> The obtained phosphonated products were characterized with different methods, starting with  $^{19}\text{F}$  NMR and  $^{31}\text{P}$  NMR spectroscopy. Spectra were only obtained for p-PSUa, p-PSUb, and p-PSUs, due to the insolubility issues of p-PSUc – PSUc is insoluble in the phosphonation agent and

could, therefore, not be phosphonated. Atanasov *et al.* showed in ref. 21 that only the *para* position of a pentafluorophenyl ring can be phosphonated. If there is a full conversion of the fluorine atom in the *para* position, only the two signals of the fluorines in the *meta* and *ortho* positions remain in the  $^{19}\text{F}$  NMR spectrum. Their integrals are in a 1 : 1 ratio. This characteristic substitution pattern was obtained for all three soluble modified PSU compounds: p-PSUa, p-PSUb, and p-PSUs. This showed the successful quantitative phosphonation of all pentafluorophenyl-containing side chains. The respective  $^{19}\text{F}$  NMR spectra are shown in Fig. 7.

Furthermore, the success of the phosphonation reaction was verified by  $^{31}\text{P}$  NMR measurements. Spectra were only obtained for p-PSUa, p-PSUb, and p-PSUs, due to the solubility issues of p-PSUc. Fig. 8 shows the  $^{31}\text{P}$  NMR spectrum of p-PSUa as an example. The spectra of p-PSUb and p-PSUs are depicted in the ESI (Fig. S1 and S2†). Within the shown spectra, only a single signal at  $-2.9$  ppm was detected, which is characteristic of the P of the phosphonic acid group. This also confirms the successful phosphonation of PSUa to p-PSUa. PSUb and PSUs were phosphonated successfully as well, yielding p-PSUb and p-PSUs.

**Thermal properties.** In addition to the polymers' structural properties, their thermal properties are important for their potential field of application. The polymers' thermal properties were determined by DSC and TGA measurements.

To investigate the influence of the introduced phosphonated side chains on the glass transition temperature  $T_g$ , the second DSC heating curve of virgin PSU was compared to those of the substituted PSUs. The second curve was used



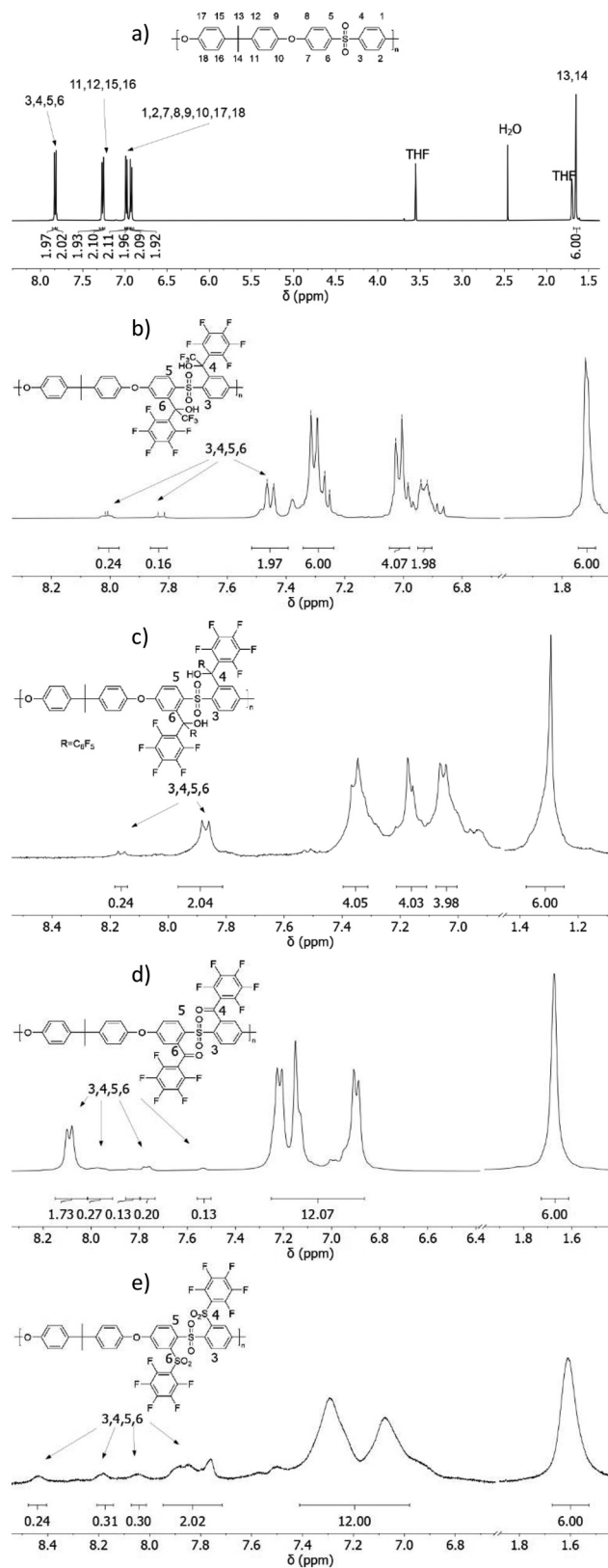


Fig. 5  $^1\text{H}$  NMR spectra of substituted PSUs. (a) Unmodified PSU, (b) PSUa, (c) PSUb, (d) PSUc, (e) PSUs, measured in THF- $d_8$  at room temperature.

Table 1 By  $^1\text{H}$  NMR spectroscopy determined degree of substitution (DOS) for the modified PSU

	PSUa	PSUb	PSUc	PSUs
DOS in %	80	88	77	58

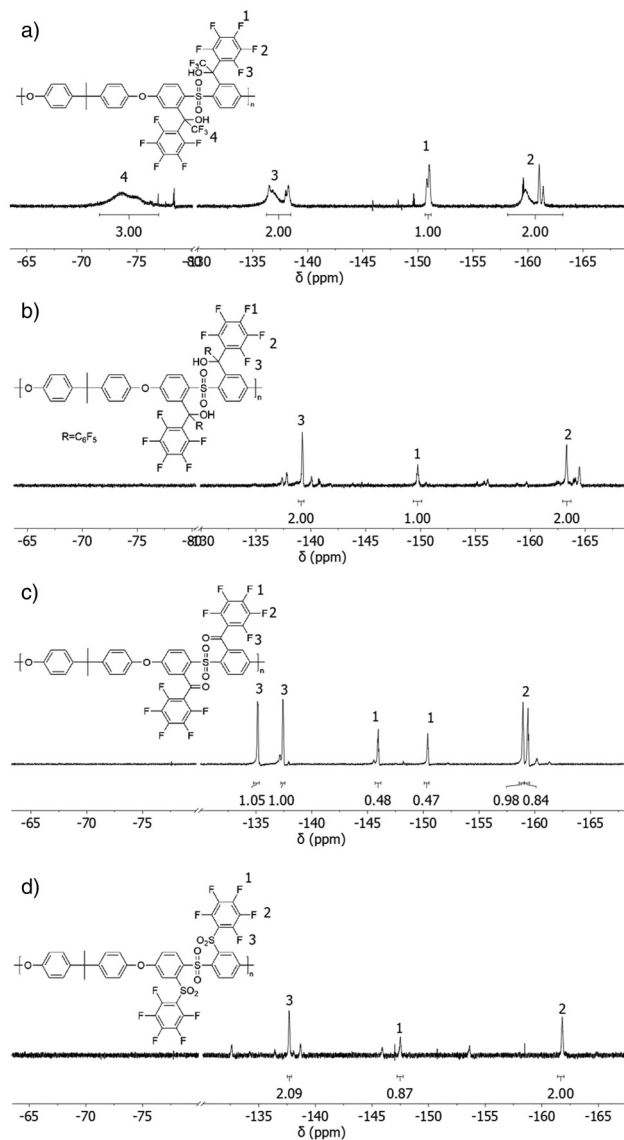


Fig. 6  $^{19}\text{F}$  NMR spectra of the four substituted PSU derivatives: PSUa (a), PSUb (b), PSUc (c), PSUs (d), measured in THF- $d_8$  at room temperature.

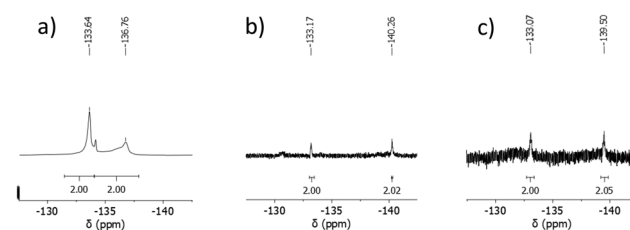


Fig. 7  $^{19}\text{F}$ -NMR spectra of p-PSUa (a), p-PSUb (b) and p-PSUs (c), measured in DMSO- $d_6$  at room temperature.



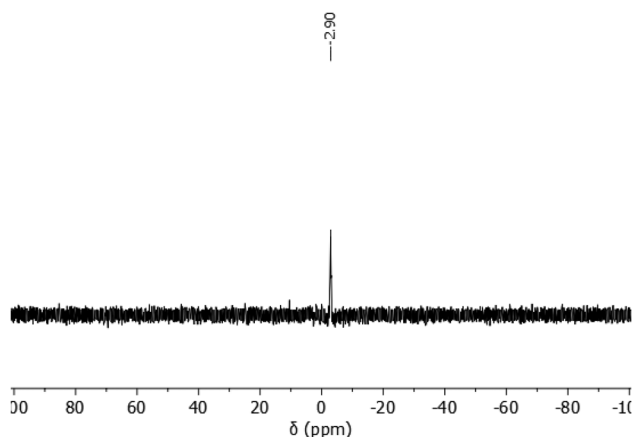


Fig. 8  $^{31}\text{P}$  NMR spectrum of p-PSUa, measured in  $\text{DMSO-d}_6$  at room temperature.

because water and solvent residuals were removed during the first heating and cooling cycle. The DSC curves of PSU and the phosphonated PSUs are depicted in the following Fig. 9.

From the DSC trace of virgin PSU, a  $T_g$  of 189 °C was determined, which is comparable to the literature.<sup>35</sup> In case large aromatic perfluorinated and phosphonated sidechains are attached to the polymeric backbone, an increasing glass transition temperature is expected for the modified polymers. In this study, the  $T_g$  for p-PSUa was determined at 215 °C and for p-PSUs at 230 °C, which proves the expected trend. The  $T_g$  of p-PSUb and p-PSUc are in the same temperature range. In summary, all four phosphonated polymers show a glass transition temperature higher than unmodified PSU (189 °C). This increase in the glass transition temperature is caused by the bulky side chains introduced to virgin PSU. The introduced aromatic rings in the side chain lead to a higher rigidity of the chains, which causes their higher glass transition temperatures.

Also, introducing phosphonic acid groups leads to an increase in the  $T_g$  since the acidic groups create a hydrogen

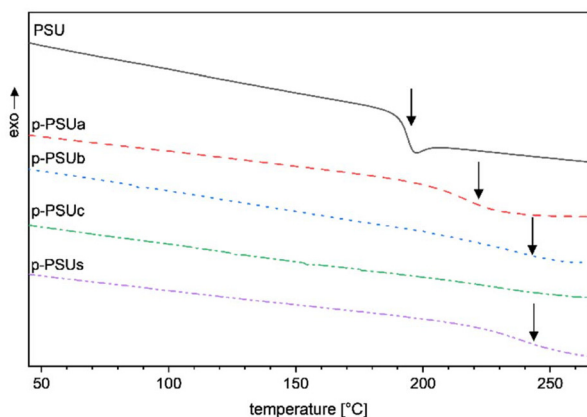


Fig. 9 DSC-traces (2nd heating cycle) of PSU, p-PSUa, p-PSUb, p-PSUc and p-PSUs.

bridge network within the macromolecular chains, which contributes to the  $T_g$  increase. For sulfonated PSU membranes, an increasing  $T_g$ , compared to unmodified PSU, has also been observed.<sup>52</sup>

Especially in the polymers' potential field of application, their thermal stability is highly important. Therefore, the thermal stability of the phosphonated synthesized materials was investigated by TGA. To be able to compare the TGA results with those of other studies, standard conditions were used (heating rate of 10  $\text{K min}^{-1}$ ). From the literature, it is well known that commercial PSU is stable up to 500 °C. Their thermal stability is in the same range regardless of whether they are exposed to air or to a nitrogen atmosphere.<sup>35,45,52</sup> In the following Fig. 10(a), the TGA traces of the phosphonated polymers are shown in comparison to virgin PSU. In Fig. 10(b), the TGA curves of unmodified PSU, PSUb, and p-PSUb are shown in comparison.

In comparison, all phosphonated polymers show a first decrease in mass of up to 100 °C, caused by remaining water residues in the polymer samples. For a sulfonated PSU derivative, a similar behaviour was observed by Karlsson *et al.*<sup>45</sup> A second decrease in mass between 2.7% and 5.0% was observed between 100 °C and 320 °C. The first mass losses in this range were caused by the release of hydration water from the phosphonic acid groups. Beginning at 200 °C, the attached phosphonic acid groups typically start forming anhydrides after the elimination of water. In a study presented by Lafitte and Jannasch, the formation of phosphonic acid anhydrides is shown for directly phosphonated PSU in a temperature range between 200 °C and 320 °C.<sup>35</sup> Bock *et al.* show that for a PSU membrane, which is phosphonated in its backbone, similar behaviour is observed below 325 °C.<sup>53</sup> This is also caused by the formation of phosphonic acid anhydrides.<sup>53</sup> In a recent study by Atanasov *et al.*, the energy barriers for the formation of different types of phosphonic acid anhydrides, *e.g.*, methyl phosphonic acid, phosphoric acid, and pentafluorophenylphosphonic acid, were discussed.<sup>32</sup> This study showed the onset of

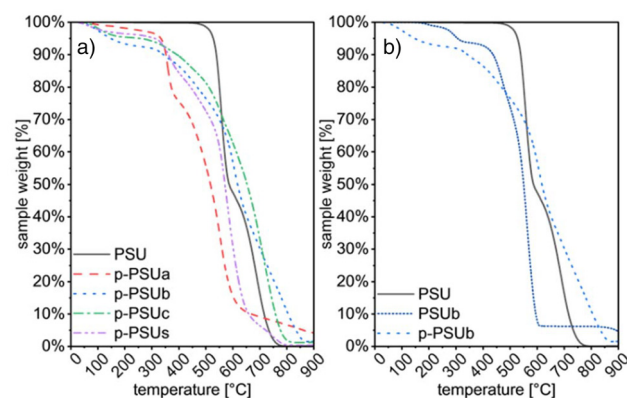


Fig. 10 (a) TGA curves of PSU, p-PSUc, p-PSUb, p-PSUs and p-PSUa under synthetic air, with a heating rate of 10  $\text{K min}^{-1}$ . (b) TGA curves of PSU, PSUb and p-PSUb under synthetic air, with a heating rate of 10  $\text{K min}^{-1}$ .



the anhydride formation at 240 °C for a pentafluorophenyl phosphonic acid.<sup>32</sup> For the PSU derivatives containing tetrafluorophenylphosphonic acid groups synthesized in this study, similar behaviour is expected. The fact that the anhydride formation of these polymeric phosphonic acids takes place only at  $T > 200$  °C makes these ionomers potential candidates for the application as electrode ionomers in HTPEMFCs, as for the related perfluoroaromatic phosphonated ionomer poly(2,3,5,6-tetrafluoro-4-phosphonic acid) the suitability for use as electrode ionomer in HTPEMFCs up to temperatures of 200 °C could be shown in the aforementioned recent study.<sup>32</sup> Beginning at a temperature of 350 °C, a decomposition of the polymers' backbones is observed. Similar behaviour was already reported for various phosphonated PSUs or PPSU.<sup>35,45,49,53–55</sup>

In Fig. 10(b), the unmodified PSU's degradation begins beyond 500 °C in a two-step degradation mechanism. In case different substituents are added to the polymer's backbone, as shown for PSUB, the beginning of the degradation was already observed at a temperature of 350 °C. In the case of the PSUB's phosphonated analogue, the evaporation of water residues and hydration water in the polymer sample was observed. Above 200 °C, the onset of formation of phosphonic acid anhydrides was observed. After that, the degradation of p-PSUB started at 350 °C, which is the same temperature range as that of PSUB.

**GPC measurements.** There is a risk of polymer degradation by the lithiation reaction. If a degradation reaction takes place, the molecular weight of the polymer will decrease, and the dispersity will increase. To compare the molecular weight before and after the lithiation step, unmodified PSU and PSUa samples were measured using THF GPC calibrated with polystyrene standards. The same was done with p-PSUa because it was also soluble in THF. The determined values for the number of average molecular weight  $M_n$ , the weight average molecular weight  $M_w$ , and the dispersity  $D$  are shown in Table 2.

The determined molecular weights were in the same range. However, the molar mass per repeating unit doubled due to the introduced side chains, which led to an apparent lower polymerization degree. On the other hand, due to the performed modification reactions, the chemical structure of the molecules became significantly changed. Adding fluorinated compounds to the polymer backbone significantly changed its polarity and hydrophilicity. This led to a different gyration radius of the polymer in solution, causing different retention times in the chromatography columns and, therefore, different

(apparent) molecular weights compared to unmodified PSU. To assess a loss in molecular weight by the modification reactions, the polydispersity index (PDI) was used. Before PSU was lithiated, the dispersity was 1.67; afterward, the polydispersity increased to 2.01. The slightly increasing PDI strongly indicates partial degradation of the backbone caused by the lithiation step. The polydispersity of the phosphonated polymer amounts to 1.56, which is lower than the PDI of PSUa (see Table 2). The phosphonation step caused this change in dispersity because the phosphonated polymer fragments with a low molecular weight became water-soluble and were washed out. For PSUB, PSUC, and PSUs, a similar trend for the polymers' dispersity was observed after adding the fluorinated compound. In total, a slight decrease in molecular weight was observed for all four modified polymers. However, the increasing dispersity and decreasing  $M_n$  do not influence further reactions and polymer properties.

**Ion exchange capacity.** Finally, the ion exchange capacities (IEC) of the phosphonated polymers were determined. Therefore, they were titrated with a sodium hydroxide solution. The theoretical values for  $IEC_{direct}$  and  $IEC_{total}$  were calculated using eqn (6) and (7). In the equation, the DOS determined by NMR-spectroscopy was used.

$$IEC_{direct,theo} = \frac{DOS \cdot \sum n_{proton,1.deprotonation}}{M_{repeating\ unit}} \quad (6)$$

$$IEC_{total,theo} = \frac{DOS \cdot \sum n_{proton,complete\ deprotonation}}{M_{repeating\ unit}} \quad (7)$$

The theoretical and experimentally determined values for the  $IEC_{direct}$  and  $IEC_{total}$  are listed in the following Table 3.

For the three phosphonated materials, p-PSUa, p-PSUB, and p-PSUs, the experimental IECs are in the same range as the theoretical ones. However, they differ slightly from the theoretical IECs, which could be caused by a differing DOS compared to the DOS determined by NMR. Furthermore, for p-PSUB and p-PSUs, an incomplete phosphonation is conceivable.

The experimental values for p-PSUC differ significantly from the theoretical ones. This strongly supports the hypothesis that the phosphonation reaction of PSUC was incomplete due to the previously discussed solubility issues.

**Solubility in organic solvents.** For their potential applicability in electrochemical cells, the materials have to be soluble for processing, e.g., in membranes. p-PSUa shows the best

**Table 2** Molecular weight distributions and Polydispersity of PSU, PSUa, and p-PSUa

	PSU	PSUa	p-PSUa
$M_{repeating\ unit}$ in $g\ mol^{-1}$	442	970	1094
$M_n$ in $g\ mol^{-1}$	43 800	38 700	44 600
$M_w$ in $g\ mol^{-1}$	73 300	78 000	69 800
$D$	1.67	2.01	1.56

**Table 3** Theoretic and experimental IECs for p-PSUa, p-PSUB, p-PSUC, p-PSUs

Polymer	Calculated		Titrated	
	$IEC_{direct}$ in $mmol\ g^{-1}$	$IEC_{total}$ in $mmol\ g^{-1}$	$IEC_{direct}$ in $mmol\ g^{-1}$	$IEC_{total}$ in $mmol\ g^{-1}$
p-PSUa	1.46	2.92	1.90	3.45
p-PSUB	2.44	4.87	2.21	4.53
p-PSUC	1.56	3.13	0.33	0.68
p-PSUs	1.10	2.20	1.04	1.65



solubility of the four materials. The good solubility in polar solvents like DMSO, DMAc, or Isopropanol is caused by the additional hydroxyl groups formed during the reaction of the lithiated PSU with perfluoroacetophenone by addition. The same is true for perfluorobenzophenone in the case of p-PSU<sub>b</sub>. However, p-PSU<sub>b</sub> has a higher fluorine content than p-PSU<sub>a</sub>, making it more hydrophobic. This explains its lower solubility in polar solvents. p-PSU<sub>c</sub> and p-PSU<sub>s</sub> contain fewer polar groups in comparison to p-PSU<sub>a</sub> and p-PSU<sub>b</sub>, which causes the low solubility in polar solvents. In the following Table 4, the solubility of the four phosphonated polymers in different selected organic solvents is listed.

#### Acid-acid blend membranes

Membranes from solely (highly) phosphonated polysulfones often show bad mechanical properties, as they tend to be brittle.<sup>35</sup> This makes them unsuitable for application as a membrane in electrochemical processes such as fuel cells, electrolyzers, and redox-flow batteries. Therefore, the synthesized polymers were cast as blend membranes together with a polymer with good film-forming and good mechanical properties. In this work, we selected another phosphonated polymer for blending, in the following named as Ter-Phos.<sup>51</sup> Thereby, almost no functionality is lost through blending, as would be the case, *e.g.*, in acid–base blends, due to electrostatic interactions of the acid group with a base (protonation of the base/ionic cross-linking between the phosphonate anion and the protonated base cation).<sup>5</sup> This blend polymer is prepared by a polyhydroxyalkylation reaction of perfluoroacetophenone with *p*-terphenyl, followed by a phosphonation reaction using the same phosphonation method as shown before.<sup>51</sup> In the ESI Fig. S11† shows the synthesis route of Ter-Phos. It was synthesized in our lab and showed good film-forming properties, high solubility, and good conductivity. Polymers of this type have been prepared recently by Kang *et al.*<sup>51</sup> However, this polymer (Ter-Phos) suffers from high water uptake and swelling, thus hindering its application as a membrane for fuel cells, electrolyzers, or redox flow batteries, as too high swelling might lead to the blocking of pore systems and mechanical pressure building up inside a cell during operation.<sup>56</sup> Blend membranes from this terphenyl polymer and our soluble phosphonated polysulfones (p-PSU<sub>a</sub>, p-PSU<sub>b</sub>, and p-PSU<sub>s</sub>) were prepared with a polymer weight ratio of 1 : 1. Despite the relatively low solubility of p-PSU<sub>b</sub> and p-PSU<sub>s</sub>, the blended membranes were readily castable. Photographs of the prepared membranes are shown in Fig. 11.

**Table 4** Solubility of PSU and p-PSUs in selected organic solvents (n = insoluble, s = soluble, (s) = partially soluble)

	DMSO	DMAc	Isopropanol	THF
PSU	n	s	n	s
p-PSU <sub>a</sub>	s	s	s	s
p-PSU <sub>b</sub>	(s)	(s)	n	n
p-PSU <sub>c</sub>	n	n	n	n
p-PSU <sub>s</sub>	(s)	n	n	n

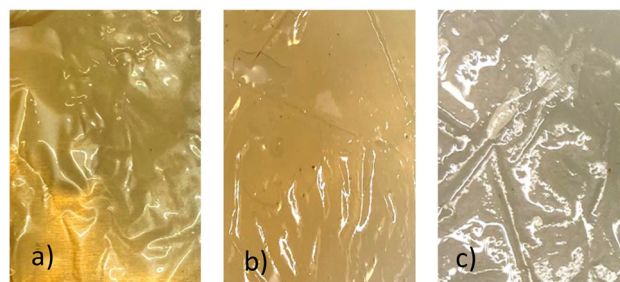


**Fig. 11** Photographs of three different blend membranes with Ter-Phos (a) p-PSU<sub>a</sub> : Ter-Phos, 1 : 1; (b) p-PSU<sub>b</sub> : Ter-Phos, 1 : 1; (c) p-PSU<sub>s</sub> : Ter-Phos, 1 : 1.

All obtained membranes were transparent, suggesting interactions (*e.g.*, hydrogen bridges) and, therefore, good miscibility between the dissolved polymers can be concluded. A reddish and yellowish colour can be seen for the pPSU<sub>b</sub> and the p-PSU<sub>s</sub> blend, respectively, caused by the different colours of the p-PSU polymers.

The polymer blend membranes were investigated in terms of water uptake, conductivity, ion exchange capacity, and stability against radicals using Fenton's test. The characterization results are shown in Table 5 and discussed below. The values for a membrane consisting of pure phosphonated terphenyl are also included in Table 5 for comparison.

The number of phosphonic acid groups attached per repetition unit follows the order p-PSU<sub>b</sub> > p-PSU<sub>a</sub> > p-PSU<sub>s</sub>. Perfluorobenzophenone is the only perfluoroaromatic compound with two pentafluorophenyl groups, which allows more phosphonic acid groups to be attached. At the same time, the p-PSU<sub>a</sub> and p-PSU<sub>s</sub> precursors have only one pentafluorophenyl moiety per side chain and, therefore, fewer sites for the subsequent phosphonation reaction. Thus, the absolute number depends on the DOS, which is lower for p-PSU<sub>s</sub> compared to p-PSU<sub>a</sub> as shown previously in Table 1. Measured and calculated IEC values reflect this order. The measured conductivity correlates with the IEC and is highest for the p-PSU<sub>b</sub> blend.

All the blend membranes show sufficient ionic conductivity. As can be seen, the pure phosphonated terphenyl membrane also shows sufficient conductivity. However, all prepared blend membranes show higher conductivities at room temperature combined with lower swelling. Particularly remarkable is the p-PSU<sub>b</sub> blend with conductivity higher than 150 mS cm<sup>-1</sup>, which hardly swells and takes up water, even after being immersed in water at 85 °C for several days.

We were able to produce mechanically stable membranes from polymers with a high phosphonation degree that maintain their high conductivity after blending and hardly swell in contact with water. The latter especially distinguishes them from other highly conductive phosphonated polysulfones, which potentially increases their applicability in electrochemical processes. Additionally, the stability against radicals determined by Fenton's test is relatively high for the blended



**Table 5** Values for IEC, thickness, water uptake, swelling, Fenton's test, and conductivity of p-PSUa, p-PSUb, p-PSUs blends, and pure Ter-Phos

	IEC <sub>total,theo</sub> [mmol g <sup>-1</sup> ]	IEC <sub>dir</sub> [mmol g <sup>-1</sup> ]	IEC <sub>tot</sub> [mmol g <sup>-1</sup> ]	Thickness [μm]	Water uptake [%]	Swelling [%]	Wt-loss Fenton's [%]	Conductivity σ [mS cm <sup>-1</sup> ]
p-PSUa	3.32	3.19	5.08	30	23	8	3	76
p-PSUb	4.29	1.98	5.23	30	0	0	11	154
p-PSUs	2.96	1.47	2.50	9	3	0	0	46
Ter-Phos	1.86	2.04	2.28	48	25	45	—	29

phosphonated membranes. Only the membrane from p-PSUb suffers from a weight loss of eleven weight percent, which is comparable to other blended phosphonated membranes. *E.g.*, Atanasov *et al.* report a seven-weight percent loss for their blended phosphonated PPFs (poly(pentafluorostyrene) and OOPBI membrane.<sup>57</sup> Our results, therefore, support the trend observed in the literature that blended membranes show higher stabilities than their pure counterpart due to the interactions between the functional groups of the blend components.<sup>58–61</sup>

## Conclusions

Within this study, a new group of PSU derivatives was synthesized. We were able to introduce four different side chains containing pentafluorophenyl moieties (perfluoroacetophenone, perfluorobenzophenone, pentafluorobenzoylchloride, pentafluorobenzenesulfonyl fluoride) to the polymer backbone. However, due to reactivity issues, sterical hindrance, and solubility issues of the substituted PSUs, we were able to introduce maximally up to two side chains per repeating unit (DOS ≈ 1). It could be shown that <sup>1</sup>H NMR spectroscopy is a suitable method for determining the degree of substitution of the polymer materials presented in this study. The substitution reactions led to materials with a high thermal stability of up to 350 °C.

Furthermore, three of the four materials (PSUa, PSUb, and PSUc) were successfully phosphonated. These polymer materials show a high thermal stability (up to 350 °C). However, they start forming phosphonic acid anhydrides above 200 °C, limiting their potential temperature range for applications such as fuel cells and electrolyzers. In addition, the phosphonated polymers have high ion exchange capacities between 1.65 mmol g<sup>-1</sup> and 4.53 mmol g<sup>-1</sup>, connected with sufficient solubility in polar solvents. In summary, these novel phosphonic acid groups containing materials are promising candidates for membranes and/or electrode ionomers in electrochemical applications such as (HT)-PEMFCs, (HT)-PEMWEs, or redox flow batteries.

First blend membranes prepared from this new class of polymers show promising conductivity and mechanical properties for application in electrochemical cells.

In ongoing work, we investigate further substitution reactions of the pentafluorophenyl group-modified PSU polymers to improve their properties in terms of proton conductivity, solubility, mechanical and thermal stability. Among the poss-

ible substitution reactions are nucleophilic substitution reactions of the F atoms of the pentafluorophenyl side chains. This opens new avenues for novel functional, high-performance polymers based on PSU.

## Author contributions

Philipp Martschin: conceptualization, methodology, resources, investigation, data curation, visualization, project administration, writing – original draft. Timo Prölls: investigation, data curation, visualization, writing – review and editing. Andreas Hutzler: investigation, data curation, visualization, writing – review and editing. Simon Thiele: writing – review and editing, supervision, funding acquisition. Jochen Kerres: conceptualization, methodology, resources, writing – review and editing, project administration, supervision.

## Data availability

The data supporting this article have been included as part of the ESI.†

## Conflicts of interest

There are no conflicts to declare.

## Acknowledgements

We acknowledge funding from the Bavarian Ministry of Economic Affairs, Regional Development and Energy, grant number 44-6665a2/132/1, and the Federal Ministry of Education and Research, grant number 03HY108A.

We gratefully acknowledge the help of Annika Schmuker, Xenia Lang, and Dominik Sämann in the characterization of the polymers and membranes presented in this study. Furthermore, we acknowledge the help of Dr Thomas Böhm for ultramicrotomy.

## References

- 1 M. Carmo, D. L. Fritz, J. Mergel and D. Stolten, *Int. J. Hydrogen Energy*, 2013, **38**, 4901.



- 2 Y. Wang, D. F. Ruiz Diaz, K. S. Chen, Z. Wang and X. C. Adroher, *Mater. Today*, 2020, **32**, 178.
- 3 S. Auffarth, W. Dafinger, J. Mehler, V. Ardizzon, P. Preuster, P. Wasserscheid, S. Thiele and J. Kerres, *J. Mater. Chem. A*, 2022, **10**, 17208.
- 4 O. Savadogo, *ChemInform*, 1998, **29**(47), DOI: [10.1002/chin.199847334](https://doi.org/10.1002/chin.199847334).
- 5 J. A. Kerres, *Fuel Cells*, 2005, **5**, 230.
- 6 P. Xing, G. P. Robertson, M. D. Guiver, S. D. Mikhailenko, K. Wang and S. Kaliaguine, *J. Membr. Sci.*, 2004, **229**, 95.
- 7 J. A. Kerres, *Polym. Rev.*, 2015, **55**, 273.
- 8 R. P. O'Hayre, S.-W. Cha, W. G. Colella and F. B. Prinz, *Fuel cell fundamentals*, John Wiley & Sons Inc, Hoboken, New Jersey, 2016.
- 9 F. Arslan, T. Böhm, J. Kerres and S. Thiele, *J. Membr. Sci.*, 2021, **625**, 119145.
- 10 Z. Wang, A. M. Buser, I. T. Cousins, S. Demattio, W. Drost, O. Johansson, K. Ohno, G. Patlewicz, A. M. Richard, G. W. Walker, G. S. White and E. Leinala, *Environ. Sci. Technol.*, 2021, **55**, 15575.
- 11 H. Brunn, G. Arnold, W. Körner, G. Rippen, K. G. Steinhäuser and I. Valentin, *Environ. Sci. Eur.*, 2023, **35**(20), DOI: [10.1186/s12302-023-00721-8](https://doi.org/10.1186/s12302-023-00721-8).
- 12 J. Miyake, R. Taki, T. Mochizuki, R. Shimizu, R. Akiyama, M. Uchida and K. Miyatake, *Sci. Adv.*, 2017, **3**, eaao0476.
- 13 N. R. Kang, T. H. Pham and P. Jannasch, *ACS Macro Lett.*, 2019, **8**, 1247.
- 14 Z. Long, J. Miyake and K. Miyatake, *ACS Appl. Energy Mater.*, 2019, **2**, 7527.
- 15 M. Adamski, N. Peressin and S. Holdcroft, *Mater. Adv.*, 2021, **2**, 4966.
- 16 M. K. Pagels, S. Adhikari, R. C. Walgama, A. Singh, J. Han, D. Shin and C. Bae, *ACS Macro Lett.*, 2020, **9**, 1489.
- 17 J. A. Kerres, D. Xing and F. Schönberger, *J. Polym. Sci., Part B: Polym. Phys.*, 2006, **44**, 2311.
- 18 M. Schuster, K.-D. Kreuer, H. T. Andersen and J. Maier, *Macromolecules*, 2007, **40**, 598.
- 19 P. Martschin, V. Atanasov, S. Thiele and J. Kerres, *ACS Polym. Au*, 2024, **4**, 492–497.
- 20 J. Chen, L. Dumas, J. Duchet-Rumeau, E. Fleury, A. Charlot and D. Portinha, *J. Polym. Sci., Part A: Polym. Chem.*, 2012, **50**, 3452.
- 21 V. Atanasov and J. Kerres, *Macromolecules*, 2011, **44**, 6416.
- 22 V. Atanasov, M. Bürger, S. Lyonard, L. Porcar and J. Kerres, *Solid State Ionics*, 2013, **252**, 75.
- 23 J.-M. Noy, Y. Li, W. Smolan and P. J. Roth, *Macromolecules*, 2019, **52**, 3083.
- 24 G. Sych, J. Simokaitiene, R. Lygaitis, E. Jatautiene, R. Pashazadeh, G. Buika and J. V. Grazulevicius, *React. Funct. Polym.*, 2019, **143**, 104323.
- 25 H. Cho, V. Atanasov, H. M. Krieg and J. A. Kerres, *Polymers*, 2020, **12**, 915.
- 26 C. D. Murphy, B. R. Clark and J. Amadio, *Appl. Microbiol. Biotechnol.*, 2009, **84**, 617.
- 27 B. Lafitte and P. Jannasch, in *Advances in Fuel Cell*, Elsevier, 2007, vol. 1, p. 119.
- 28 D. J. Jones and J. Rozière, *J. Membr. Sci.*, 2001, **185**, 41.
- 29 *Fundamentals and performance of low temperature fuel cells*, ed. C. Hartning and C. Roth, Woodhead Pub, Oxford, 2012.
- 30 *High Temperature Polymer Electrolyte Membrane Fuel Cells: Approaches, Status, and Perspectives*, ed. Q. Li, D. Aili, H. A. Hjuler and J. O. Jensen, Springer, Cham, 2016.
- 31 C. Vogel and J. Meier-Haack, *Desalination*, 2014, **342**, 156.
- 32 V. Atanasov, A. S. Lee, E. J. Park, S. Maurya, E. D. Baca, C. Fujimoto, M. Hibbs, I. Matanovic, J. Kerres and Y. S. Kim, *Nat. Mater.*, 2021, **20**, 370.
- 33 M. D. Guiver, J. W. Apsimon and O. Kutowy, *J. Polym. Sci., Part C: Polym. Lett.*, 1988, **26**, 123.
- 34 V. L. Rao, *J. Macromol. Sci., Part C: Polym. Rev.*, 1999, **39**, 655.
- 35 B. Lafitte and P. Jannasch, *J. Polym. Sci., Part A: Polym. Chem.*, 2005, **43**, 273.
- 36 *Fuel Cells II*, ed. G. G. Scherer, Springer Berlin Heidelberg, Berlin, Heidelberg, 2008.
- 37 P. Zschocke and D. Quellmalz, *J. Membr. Sci.*, 1985, **22**, 325.
- 38 P. Jannasch, *Fuel Cells*, 2005, **5**, 248.
- 39 M. D. Guiver, S. Croteau, J. D. Hazlett and O. Kutowy, *Br. Polym. J.*, 1990, **23**, 29.
- 40 M. D. Guiver, P. Black, C. M. Tam and Y. Deslandes, *J. Appl. Polym. Sci.*, 1993, **48**, 1597.
- 41 J. Kerres, W. Cui and S. Reichle, *J. Polym. Sci., Part A: Polym. Chem.*, 1996, **34**, 2421.
- 42 *Membrane formation and modification*, ed. I. Pinnau, American Chemical Society, Washington, DC, 2000.
- 43 J. Kerres, A. Ullrich and M. Hein, *J. Polym. Sci., Part A: Polym. Chem.*, 2001, **39**, 2874.
- 44 B. Lafitte, L. E. Karlsson and P. Jannasch, *Macromol. Rapid Commun.*, 2002, **23**, 896.
- 45 L. E. Karlsson and P. Jannasch, *Electrochim. Acta*, 2005, **50**, 1939.
- 46 J. C. Persson, K. Josefsson and P. Jannasch, *Polymer*, 2006, **47**, 991.
- 47 B. Lafitte, M. Puchner and P. Jannasch, *Macromol. Rapid Commun.*, 2005, **26**, 1464.
- 48 J. Parvole and P. Jannasch, *J. Mater. Chem.*, 2008, **18**, 5547.
- 49 J. Parvole and P. Jannasch, *Macromolecules*, 2008, **41**, 3893.
- 50 J. Kerres, A. Ullrich, T. Häring, M. Baldauf, U. Gebhardt and W. Preidel, *J. New Mater. Electrochem. Syst.*, 2000, **3**, 229–239.
- 51 N. R. Kang, T. H. Pham, H. Nesterstedt and P. Jannasch, *J. Membr. Sci.*, 2021, **623**, 119074.
- 52 F. Lufrano, G. Squadrito, A. Patti and E. Passalacqua, *J. Appl. Polym. Sci.*, 2000, **77**, 1250.
- 53 T. Bock, R. Mülhaupt and H. Möhwald, *Macromol. Rapid Commun.*, 2006, **27**, 2065.
- 54 N. Y. Abu-Thabit, S. A. Ali and S. M. Javaid Zaidi, *J. Membr. Sci.*, 2010, **360**, 26.
- 55 H. Tang, K. Geng, Y. Hu and N. Li, *J. Membr. Sci.*, 2020, **605**, 118107.
- 56 Y. Zhou, G. Lin, A. J. Shih and S. J. Hu, *J. Power Sources*, 2009, **192**, 544.



- 57 V. Atanasov, D. Gudat, B. Ruffmann and J. Kerres, *Eur. Polym. J.*, 2013, **49**, 3977.
- 58 J. Kerres and V. Atanasov, *Int. J. Hydrogen Energy*, 2015, **40**, 14723.
- 59 E. Bülbül, V. Atanasov, M. Mehlhorn, M. Bürger, A. Chromik, T. Häring and J. Kerres, *J. Membr. Sci.*, 2019, **570–571**, 194.
- 60 J. Kerres, F. Schönberger, A. Chromik, T. Häring, Q. Li, J. O. Jensen, C. Pan, P. Noyé and N. J. Bjerrum, *Fuel Cells*, 2008, **8**, 175.
- 61 D. Yazili, E. Marini, T. Saatkamp, A. Münchinger, T. de Wild, L. Gubler, G. Titvinidze, M. Schuster, C. Schare, L. Jörissen and K.-D. Kreuer, *J. Power Sources*, 2023, **563**, 232791.

